Universidad de Alcalá
BIBLIOTECA

Document downloaded from the institutional repository of the University of Alcala: http://ebuah.uah.es/dspace/

This is a postprint version of the following published document:

Palomar, I., Barluenga, G., Ball, R. J. & Lawrence, M. (2019) "Laboratory characterization of brick walls rendered with a pervious lime-cement mortar", *Journal of Building Engineering,* vol. 23, pp. 241-249

Available at https://doi.org/10.1016/j.jobe.2019.02.001

© 2019 Elsevier

Universidad de Alcalá

(Article begins on next page)

This work is licensed under a

Creative Commons Attribution-NonCommercial-NoDerivatives 4.0 International License.

Laboratory characterization of brick walls rendered with a pervious lime-cement mortar

I. Palomar [a,1], **G. Barluenga** [a], **R.J. Ball** [b], **M. Lawrence** [b]

[a] Department of Architecture, University of Alcala, Spain

[b] BRE Center for Innovative Construction Materials, Department of Architecture & Civil Engineering, University of Bath, UK

ABSTRACT

A laboratory study investigating important thermal retrofitting solutions for simple and double (cavity) brick walls is presented. Test walls were modified using materials of current interest including an external pervious lime-cement mortar render and insulation board prior to evaluation. Laboratory simulations of steady-state winter and summer scenarios were performed using apparatus comprising two opposing climate chambers. Temperature, relative humidity and heat flux rate were monitored with surface sensors every 10 minutes until stabilization on each wall type, retrofitting solution and climate scenario. The temperature and relative humidity profiles, heat flux, surface temperature difference, thermal conductance, condensation risk and stabilization times were assessed. Comparisons between simple and double (cavity) brick walls showed significant differences and a high condensation risk in the non-ventilated air cavity of the double wall. The pervious lime-cement mortar render enhanced substantially the thermal performance of the single wall although increased the condensation risk of the double (cavity) wall. As expected, the insulation layer reduced the thermal conductance of the wall, although the improvement in a summer scenario was considerably lower than in winter. The different performance observed between winter and summer steady-state conditions emphasized the importance of the heat and mass transfer coupling effect. Therefore, this work proves that effective retrofitting depends on materials, wall layouts and climate conditions. These experimental results provide essential knowledge about assessing the effects of common retrofitting solutions especially under hot-dry summer scenarios.

KEYWORDS

Brick walls; Pervious mortar; Retrofitting; Thermal performance; Heat and moisture transfer.

[1] Corresponding author. Departamento de Arquitectura. Escuela de Arquitectura, Universidad de Alcalá, C. Santa Úrsula, 8. Alcalá de Henares, 28801 Madrid, Spain. Tel.: +34 918839239; fax: +34 918839246 - *E-mail address*: irene.palomar@uah.es (I.Palomar)

1 Introduction

Existing dwelling buildings are part of a large building stock characterized by a large energy consumption, according to current energy efficiency standards [1, 2]. In the case of Spain, around 70% of the dwelling stock was built before the first national energy efficiency regulation was put into force in 1979, and 45% was built between 1960 and 1980 [3]. Due to its low energy efficiency, the residential sector is responsible for over 20% of the total energy consumption in Spain [4]. Thus, energy efficiency improvement has become a main concern and effective retrofitting techniques and materials are required.

Retrofitting this dwelling stock, which includes historical and traditional buildings, is a balance among reducing energy consumption, improving long-term building performance and satisfying today's functional requirements [5]. The most common (and cheapest) retrofitting solution for those buildings is an External Thermal Insulation Composite System (ETICS) [2]. However, some issues arise due to the embodied energy increase of traditional walls [6] and its low adaptability to specific insulation thickness and hygrothermal performance [7] that could produce moisture accumulations and organic growth in cold climates [8] and overheating in summertime [9]. On the other hand, façade retrofitting often requires the substitution of deteriorated traditional mortars, which becomes an opportunity to fulfill the nowadays building requirements through the design of new mortar coatings [10, 11, 12, 13]. Considering this, new pervious lime-cement mortars (PLCM) with short cellulose fibers (CF) have been designed to improve thermal and acoustic properties, fulfilling conservation, aesthetic, structural, service-life and construction issues [14, 15]. The main characteristic of PLCM is the lack of fine aggregate particles that creates an interconnected void network where spherical aggregate particles are surrounded by a shell of lime-cement paste and CF [16].

According to the literature [17], brick wall façades of those residential buildings can have one or two brick layers. Double walls were traditionally built with an intermediate non-ventilated air cavity. Due to the 70's energy crisis, a thermal insulation layer of 30-40 mm was typically incorporated between the brick layers, filling the air cavity. Before 1960, one layer brick walls were a common solution, using solid bricks, and lately 360 mm perforated bricks or even 120 mm hollow bricks.

As the new energy efficiency regulations come into force [1, 5], many brick wall facades were retrofitted with different types of renders, achieving various levels of effectiveness depending on the wall typology and climate scenario. Some studies reproduce common typologies and climate conditions, focusing on factors affecting thermal performance of lime or cement mortars, such as moisture content dependency [18, 19], the interface phenomena in a multiple layer wall [20] or the overestimation of traditional materials and wall properties, due to a lack of experimental data for computer models [21]. However, these results cannot be extrapolated to

other climate conditions as those characterized by high seasonal variations, large diurnal daily ranges and high temperature and low relative humidity on summer days, which are typical of Southern Europe's climate [22], since operating conditions affect the thermal performance of standard and retrofitted walls [6].

The hygrothermal performance of building materials and façade walls can be studied using mathematical and computer models simulating the coupled effect of heat and moisture transfer through multilayer walls [23, 24, 25]. However, these algorithms require reliable material properties from laboratory characterization [26] or involve a long-term monitoring to ensure reliability and overestimate pre-standard buildings performance [27]. Other alternative methods such as outdoor test cells or on-site assessment methods have been reported, which allow consideration of dynamic boundary conditions [28, 29]. Laboratory simulation tests have also been widely used, creating "artificial on-site conditions" with climatic chambers and reproducing either quasi steady-state or dynamic scenarios [7, 30, 31, 32, 33]. Considering both the full-scale and laboratory tests, climate scenarios can be easily applied to any wall layout in the laboratory-controlled conditions to estimate its hygrothermal behavior [34]. Only few studies used a complete approach that included laboratory tests, outdoor test cells, dynamic identification techniques, model calibration, simulation and full-scale building monitoring [35].

This paper presents an experimental program aimed to investigate the effect of a pervious lime-cement mortar render (PLCM) with and without an insulation board for thermal retrofitting of simple and double (cavity) brick walls. Winter and summer steady-state scenarios were simulated using two climatic chambers applied on both sides of the test walls with and without rendering. Temperature, relative humidity and heat flux were monitored. The effectiveness of the retrofitting solution for each wall type, retrofitting solution and climate scenario was assessed.

2 Experimental program

Two wall types, simple and double (cavity) brick walls, two retrofitting solutions including pervious lime-cement mortars (PLCM) and two climate scenarios, steady state winter and summer, were experimentally characterized. The walls and scenarios used in this study reproduce common constructive typologies and climate conditions characterized by high seasonal variations and high temperature and low relative humidity on summer. Two climate chambers were placed opposite one to another on each side of the testing wall to simulate indoor and outdoor conditions. Temperature, relative humidity and heat flux sensors were used to monitor hygrothermal parameters and the measurements were recorded every 10 minutes for at least 24 hours after steady-state conditions were reached. Temperature (T) and relative humidity (RH) profiles, density of heat flux rate (HF), surface temperature difference (ΔT), thermal conductance (Λ), condensation risk (CR) and

stabilization time (t_s) were analyzed. The experimental results were used to compare the different brick walls, retrofitting solutions and climate scenarios.

2.1 Materials

The materials used in the study were:

- Three clay bricks (Category II, HD):
    - vertically perforated bricks (VPB) of 215 x 102.5 x 65 mm,
    - frogged bricks (FB) of 215 x 102.5 x 65 mm,
    - solid bricks (SB) of 215 x 102.5 x 35 mm.
- Four binders:
    - an air lime class CL 90-S,
    - a white cement CEM I 52.5 R –SR5,
    - a cement type CEM II/B-V/32.5R,
    - a one coat gypsum plaster class B4/20/2.
- Two aggregates: a siliceous sand (0-4 mm) and a gap-graded limestone sand (2-3 mm).
- Short cellulose fibers of length 1 mm - Fibracel® BC-1000 (Ø20μm) - supplied by Omya Clariana S.L.
- Rigid insulation board of polyisocyanurate foam and low emissivity foil facings (X) of 50 mm.

The binder materials were used to produce a retrofitting render (R), a Plaster (P) and a Joint mortar (J), prepared as follows:

- Retrofitting render (R): Pervious lime-cement mortar (PLCM) with gap-graded limestone sand (1:1:6 by volume lime/cement/sand ratios), cellulose fibres (1.5% of the total dried mortar's volume) and 0.94 water to binder ratio (w/b). This mixture was selected out of twelve evaluated in a previous study due to the particular suitability for external rendering when considering the technical, functional and performance requirements [14]. The use of cellulose fibers in PLCM improved the thermal and acoustic performance - the lowest thermal conductivity coefficient and the highest noise reduction was observed from a previous study as both paste thickness and active void size were modified [16].
- Plaster (P): A one coat gypsum plaster with w/b = 0.45
- Joint mortar (J): Cement mortar with continuous siliceous sand (1:6 by volume) and w/b =1

Table 1 summarizes some materials' properties as bulk density (ρ), moisture-dependent water vapor diffusion resistance factor (μ), thermal conductivity (λ), specific heat (cp) and thermal diffusivity (α). Thermal diffusivity (α) was calculating according to Eq. (1) [36]:

$$\alpha = \frac{\lambda}{\rho \cdot c_p} \quad (1)$$

where λ is the thermal conductivity of the material, ρ is bulk density and c_p specific heat.

The retrofitting render (R) was previously characterized and showed a suitable thermal and acoustic performance [14, 15, 16]. The gypsum plaster thermo-physical properties were experimentally characterized. Nominal properties for bricks [37] and insulation board provided by the manufacturers were considered, although slight differences can be expected due to the effect of temperature, moisture and aging [38].

2.2 Façade brick wall layouts

Five wall configurations, three single walls and two double (cavity) walls, were fabricated. Fig. 1 shows the 450 x 440 mm brick wall cross-sections.

The reference single wall (REF(S)) was built with one 103 mm thick layer of vertically perforated bricks (VPB) and a joint cement mortar (J), while the reference double (cavity) wall (REF(D)) was built with two layers, 35 mm solid bricks (SB) and 103 mm frogged bricks (FB), with a 40 mm non-ventilated air cavity (A) in between. The interior side of both walls was coated with 15 mm gypsum plaster (P).

Then, the external side of both walls was rendered with a 25 mm pervious lime-cement mortar (R), named REF(S)+R and REF(D)+R respectively. The single wall was also retrofitted combining a 50 mm thick thermal insulation board (X) with the pervious lime-cement render (R), noted as REF(S)+X+R. A polyisocyanurate (PIR) insulation panel was selected to reduce insulation thickness while complying with energy efficiency standards [39, 40]. Besides, PIR has the best fire resistance among foam plastics [39].

The design thermal conductance (Λ_c) of the wall layouts was calculated according to Eq. (2) [36]:

$$\Lambda_C = \frac{1}{\sum_j \frac{d_j}{\lambda_j}} \quad (2)$$

where λ is the thermal conductivity and d is the thickness of each layer (j) in Table 1.

2.3 Experimental methods

Fig. 2 shows the experimental setup designed for this study. The walls were built inside a plywood framework, sealed and thermally isolated with polyisocyanurate foam to allow a one-dimensional heat and moisture flux. Samples were stored under laboratory conditions at 22 ± 2ºC and 60 ± 10% RH until testing. The framework with the wall was then placed between two climate chambers simulating the effect of different climate conditions on the walls. Temperature (T) and relative humidity (RH) were set using two TAS MTCL-135 climate

chambers with HMI Control Systems which was used to produce heat and moisture flux that simulated winter and summer scenarios. The water vapor density (v) for each scenario was estimated according to ISO 13788 [40]. The interior conditions were set at 23ºC and 50 ±5% RH (v = 0.0103 ± 0.001 kg/m^3) and the exterior conditions were 12ºC, 80±5% RH (v = 0.0085 ± 0.0005 kg/m^3) for winter and 31ºC, 40±5% RH (v = 0.0128 ± 0.002 kg/m^3) for summer. These conditions were selected to simulate climates with high seasonal variations and high temperature and low RH in summer.

K type thermocouples and relative humidity sensors (HIH4000) were used to monitor the interior of the chambers and the surfaces of all the layers of the walls at 10 minute intervals. A heat flux sensor (HFP01 by Hukseflux) was placed in the interior side of the walls. The operational error in the heat flux meter (HFM) was calculated as 10% to 22%, according to ISO 9869 [42]. Temperature (T), relative humidity (RH) and density of heat flux rate (HF) were monitored on the walls and the results were analyzed after a steady-state regime was reached. Afterwards, laboratory-experimental thermal conductance (Λ), risk of surface and interstitial condensation (CR) and transition time (t_s) were calculated and used to compare single and double walls with and without retrofitting solutions in winter and summer scenarios. Laboratory-experimental thermal conductance (Λ) of the wall layouts was estimated using the ratio between the mean density of heat flow rate (HF) and mean temperature difference between the interior ($T_{s,i}$) and exterior ($T_{s,e}$) surfaces after a steady-state regime was reached over a long enough period of time [41,42].

3 Experimental results

Two wall types, simple and double cavity brick walls, two retrofitting solutions with an exterior pervious lime-cement mortar render with and without an insulation board, and two steady-state climate scenarios, winter and summer, were experimentally characterized.

3.1 Laboratory characterization of simple brick walls

Temperature (T) and relative humidity (RH) cross-sections of the single walls in steady-state winter and summer scenarios are plotted in Fig. 3. It can be observed that the addition of exterior pervious lime-cement mortar render and an insulation board produced different effects.

In the winter scenario, the temperature difference (ΔT) for the brick layer (W_1) was 6.45 ºC in the reference single wall REF(S), whereas ΔT were 3.95 and 0.52 ºC for rendered (REF(S)+R) and insulated (REF(S)+X+R) single walls respectively. The highest RH values were found on the exterior pervious lime-cement mortar

render (R) both in REF(S)+R and REF(S)+X+R walls. However, RH was lower than 100% and there was no surface or interstitial condensation in any single wall in the winter scenario.

In the summer scenario, the addition of exterior pervious lime-cement mortar render (R) reduced the temperature difference of the brick layer (W_1) from 4.20 ºC to 2.47 ºC. In addition, the interior plaster (P) also showed lower temperatures. When an insulation board (X) was added, its temperature difference was 5.68 ºC and almost zero in the other layers. RH cross-sections showed similar values for both REF(S) and REF(S)+R. On the other hand, the addition of an insulation board (X) increased RH between W_1 and X layers, although no surface or interstitial condensation was recorded.

3.2. Laboratory characterization of double (cavity) brick walls

Fig. 4 shows temperature (T) and relative humidity (RH) cross-sections of the double (cavity) walls measured in steady-state winter and summer scenarios, showing the effect of a non-ventilated air cavity (REF(D)) and an exterior pervious lime-cement mortar render (REF(D)+R).

REF(D) temperature cross-section in the winter steady-state scenario showed that the interior brick layer (W_2), the non-ventilated air cavity (A) and the exterior brick layer (W_3) had temperature differences (ΔT) of 1.39, 4.21 and 3.53 ºC, respectively. In the case of REF (D)+R, the render (R) showed a ΔT of 2.26 ºC and halved the temperature difference of the non-ventilated air cavity to 2.20 ºC. The brick layers (W_2 and W_3) and plaster (P) had similar temperatures in both walls. The RH cross-section of REF(D) showed a high relative humidity in the air cavity (A) and interstitial condensation occurred. Nevertheless, no surface condensation in winter conditions was recorded. The same happened on the rendered wall, REF(D)+R: interstitial condensation occurred, especially in the exterior brick layer (W_3), but no surface condensation was recorded.

In the summer scenario, the interior brick layer (W_2), the non-ventilated air cavity (A) and the exterior brick layer (W_3) had a temperature differences (ΔT) of 1.95, 1.54 and 4.38 ºC, respectively. Therefore, the non-ventilated air cavity (A) had less effect on temperature cross-section in summer than in winter, whereas the external brick layer (W_3) showed the higher thermal difference. The addition of exterior PLCM render (R) reduced the temperature difference of the interior brick layer (W_2) and the non-ventilated air cavity (A) to one half and the external brick layer (W_3) to one third which was the lowest recorded in this layer. The render layer had a ΔT of 3.55 ºC, which corresponded to 44% of the total temperature difference while in the winter scenario a temperature difference of only 22% was reached. Therefore, the rendering produced a larger improvement on double walls in summer than in winter. RH of REF(D) was also different in summer than in the winter scenario, as the brick layer (W_3) condensed water in summer. Moreover, the addition of the rendering (REF(D)+R) extended the area affected by interstitial condensation to the air cavity (A) and the external brick

layer (W_3). However, this cannot be considered a problem because the condensed water can easily evaporate in summer conditions.

4 Analysis and discussion

The laboratory data was used to compare the different brick walls, retrofitting solutions and scenarios. Density of heat flux rate (HF), surface temperature difference (ΔT), thermal conductance (Λ), stabilization time ($t_{s,HF}$; $t_{s,\Delta T}$) and condensation risk (CR) during steady-state winter and summer conditions were analyzed and the experimental results summarized in Table 2. One-dimensional heat and moisture flux through the walls can be assumed for both steady-state scenarios. In winter, the heat and moisture transfer occurred from the inside to the outside (outwards), while in summer, the flux was from the outside to the inside (inwards).

4.1 Effect of the non-ventilated air cavity on the wall performance

Table 2 shows the laboratory measurements of density of heat flux rate (HF) and surface temperature difference (ΔT) of single and double walls. It can be observed that the ΔT value reached an asymptotic situation earlier than HF ($t_{s,\Delta T} < t_{s,HF}$). The larger difference in double walls can be partially attributed to the water condensed in the non-ventilated air cavity (Fig. 4). HF stabilization occurred after the moisture flow ended, due to the heat and mass transfer coupling effect.

The effect of the non-ventilated air cavity on the wall performance can be evaluated comparing the heat flux (HF), surface temperature difference (ΔT), thermal conductance (Λ), stabilization time ($t_{s,\Delta T}$; $t_{s,HF}$) and condensation risk (CR) during steady-state winter and summer conditions (Table 2). Double brick walls reduced the heat flux of single walls in both scenarios by almost three times. This can be explained by the low thermal conductivity of the still air in the non-ventilated air cavity (A). In addition, the surface temperature difference was around 1ºC higher in the double compared to the simple wall. Although the non-ventilated air cavity (A) reduced significantly the thermal conductance, a high condensation risk was observed in all scenarios and the air cavity would require drainage. Concerning the stabilization time of HF, REF(D) doubled the time of REF(S) to stabilize in winter, whereas both walls stabilized almost simultaneously in summer. The differences of $t_{s,HF}$ can be attributed to the condensed water and moist air in the non-ventilated air cavity in winter and summer which would modify the materials' specific heat and thermal conductivity, increasing heat storage [43].

4.2 Assessment of the retrofitting solutions

In this section, the effect of a pervious lime-cement mortar render (R) and an insulation board (X) on single and double brick walls was evaluated.

4.2.1 Effect of pervious lime-cement mortar render (R)

Rendering the simple and double brick walls with a pervious lime-cement mortar produced two effects related to the heat and moisture transfer. On one hand, the insulation capacity of the mortar reduced the measured thermal conductance (Λ) (Table 2). This reduction was larger in the simple wall compared to the double wall and also in the summer conditions compared to the winter conditions. In addition, the rendered double wall REF(D)+R showed a similar thermal conductance as the insulated single wall REF(S)+X+R in the summer scenario.

The second effect was related to the low vapor permeability of the mortar which modified moisture transfer. The consequences on double brick walls can be summarized as an increase of condensation inside the non-ventilated air cavity and an extension of the layers affected by interstitial condensation risk (Fig.4).

The combined effect of the render on the heat and moisture transfer also delayed the heat flux stabilization time ($t_{s,HF}$) in all scenarios and wall types, except for the double wall in winter conditions. REF(D)+R in summer conditions showed the highest heat flux stabilization time. The explanation can be found on its insulation capacity and low permeability jointly with its thermal inertia, as the moisture content modified specific heat and increased heat storage of building materials [43].

Accordingly, the incorporation of the render layer on the external side of the walls produced a reduction of the energy needed to keep the interior conditions which would mean lower energy consumption for air conditioning. It would also reduce the thermal variations of the brick layers which would improve their dimensional stability, reducing the cracking risk of the wall under severe climate variations and would improve wall durability [9]. However, the thermal difference between render and brick wall would require a good adherence between the mortar and the brick layer.

4.2.2 Effect of the insulation board (X)

The incorporation of a thermal insulation board, jointly with the mortar render, on the exterior side of the single wall as an improved retrofitting solution produced a significant reduction of heat flux (Table 2), as expected [44]. However, the overall improvement depended on the climate conditions: the thermal conductance measured (Table 2) in the winter scenario was half of the design value (Fig. 1), remarkably better than

expected, while in the summer scenario the value was doubled. Therefore, the effect of the insulation board was strongly reduced in summer conditions. Those results agree with the literature: differences between experimental and design values when insulation was included [21] and those differences are larger in summer conditions than in winter [39].

A secondary effect of the insulation board was the vapor barrier effect due to its extremely low vapor permeability. This property significantly reduced heat flux stabilization time, especially in winter scenario, reaching a value similar to the rendered double wall (REF(D)+ R) in winter which was highly affected by condensation. This can be related to the reduction of vapor transfer jointly with the flux and moisture direction in each case (outwards in winter and inwards in summer), and it could lead to an increased risk of damage in the render layer in winter and the plaster in summer due to moisture accumulation and of interfacial mechanisms [20].

4.3 Temperature (T), relative humidity (RH) and heat flux (HF) stabilization time

Stabilization began in the external layers and was reached later in the internal layers, both in winter and summer scenarios, except for the non-ventilated air cavity due to its lack of thermal inertia. It was observed that the time to reach a steady-state regime depends on the wall type, retrofitting solutions and climate scenario (Table 2 and 3). The single brick walls took at least 18 hours to stabilize RH in summer scenario. On the other hand, only REF(S)+X+R showed a similar behaviour (14 hours) in winter. T values, which stabilized the last in the case of double cavity brick walls, required at least 12 hours in all the climate scenarios.

In general, single walls stabilized slightly faster in winter than in summer. When the three single wall layouts were compared (Table 3), REF(S)+X+R exhibited the lower stabilization time of HF, followed by REF(S) and REF(S)+R. Consequently, REF(S)+X+R took less time to reach an equilibrium compared to other single walls. In double walls (Table 3), REF(D)+R showed the longest stabilization time in summer for both T and HF, but not for RH. However, this wall was the fastest to stabilize HF in winter, with stabilization times shorter than those obtained for single walls.

Regarding the three parameters evaluated, RH stabilized before T and HF, with the exception of REF(S) in summer and the thermally insulated single wall in both scenarios, REF(S)+X+R, which showed the opposite. In this case (REF(S)+X+R), the delay on RH values in Table 3 corresponded to insulation-render interlayer (X-R) in winter and to plaster-internal brick interlayer (P –W_1) in summer. As far as there were peaks on RH and not on temperature stabilization time data (Table 3), it can be assumed that this change was due to the vapor barrier effect of the insulation board. In double walls, HF always stabilized before T. The heat and mass transfer coupling effect can explain why heat flow stabilization occurred after the moisture flow ended.

4.4 Effective brick wall retrofitting in different climate scenarios

The experimental results pointed out that the simple and double brick walls and retrofitting solutions behaved different in winter and summer scenarios, which agrees with previous studies [45]. Thermal conductance measured in the laboratory tended to be higher in winter than in the summer scenario and different from the design values. Heat flux stabilization time was longer in summer than in winter scenario. The effect of climate conditions also depended on the layers affected by interstitial condensation in double brick walls, due to a heat and moisture transfer coupling effect which would modify the materials' specific heat, thermal conductivity and heat storage capacity [43]. It would be a positive effect in summer (inwards heat and moisture transfer) due to the increase of thermal capacity, but a negative effect in winter (outwards transfer) due to the increase of thermal conductivity.

The use of an external insulation board on simple brick walls reduced the heating demand significantly in winter. However, the insulation capacity depended on the climate conditions and was strongly reduced in summer, as reported previously [39]. On the other hand, the use of the pervious lime-cement mortar render on the external side of the double brick walls produced a reduction of the cooling energy needed to maintain the interior conditions in summer which would mean less energy consumption in air conditioning [47, 34]. Therefore, the effectiveness of a retrofitting solution depends on both the material properties and the climate conditions.

Consequently, heating and cooling demand would be underestimated if the heat and moisture coupling effect is not considered. This is in agreement with other authors who highlighted the need of different strategies than thermal insulation to enhance the thermal performance of buildings in climates with a hot summer [46].

5 Conclusions

This paper presents a laboratory characterization of two wall types, simple and double (cavity) brick walls, two retrofitting solutions, a pervious lime-cement mortar render with and without an insulation board, and two climate scenarios, steady state winter and summer simulated using two climate chambers. The experimental program measured temperature, relative humidity (RH) and heat flux rate (HF). Laboratory-experimental thermal conductance, surface and interstitial condensation and temperature, RH and heat flux stabilization time were calculated. The main findings of the study are:

- The measured results of experimental thermal conductance were different from the calculated values and depended on the climate conditions.

- The hygrothermal stabilization of the wall occurred first on the outer layers and afterwards in the inner layers. RH stabilized first, then temperature and HF stabilized the last, due to the heat and moisture coupling effect.
- Double (cavity) brick walls showed better thermal performance than simple walls due to the non-ventilated air cavity. However, double brick walls showed a high condensation risk in both winter and summer scenarios and the air cavity would require drainage.
- The use of an exterior pervious lime-cement mortar render (R) improved the thermal performance of both single and double walls, delaying the heat flux stabilization time. Although, it can increase interstitial condensation in double walls due to the render's low vapor permeability.
- The use of an external insulation board (X) improved the thermal performance in winter conditions, significantly reducing the heat flux and, therefore, the energy required for heating. However, the behavior in summer scenario was significantly worse than expected.
- The differences between expected and measured results can be attributed to the effect of moisture transfer on heat transfer and wall thermal properties. Therefore, the effectiveness of a retrofitting solution depends on both the material properties, and the climate conditions.

Acknowledgments

The authors wish to acknowledge the help of Dr Eshrar Latif and Dr Daniel Maskell, and the contribution on the testing preparation of the technical staff of the Engineering & Design Technical Services at the Department of Architecture and Civil Engineering, University of Bath. Some of the components were supplied by Omya Clariana S.L.

Funding

Financial support for this research was provided by the Trainee Research Personnel Mobility Grant (Movilidad PIF-UAH 2015) and Grant for training of Lecturers (FPU-UAH 2013), funded by the University of Alcala.

Declarations of interest

None

References

[1] Directive 2010/31/EU of the European Parliament and of the Council of 19 May 2010 on the energy performance of buildings. Official Journal of the European Union, nº L 153, of 18 June 2010

[2] Ma Z, Cooper P, Daly D, Ledo L (2012) Existing building retrofits: Methodology and state-of-the-art. Energy Build 55: 889-902. https://doi.org/10.1016/j.enbuild.2012.08.018

[3] "Owner-occupied dwellings by type and year of construction of the building" (2001) Eurostat database, European Commission, Luxembourg. http://ec.europa.eu/eurostat/web/products-datasets/product?code=cens_01ndpercons. Accessed 10 May 2016

[4] Pérez-Lombard L, Ortiz J, Pout C (2008) A review on buildings energy consumption information. Energy Build 40(3):394-398. https://doi.org/10.1016/j.enbuild.2007.03.007

[5] Webb AL (2017) Energy retrofits in historic and traditional buildings: A review of problems and methods. Renewable Sustainable Energy Rev 77:748-759. https://doi.org/10.1016/j.rser.2017.01.145

[6] Kyriakidis A, Michael A, Illampas R, Charmpis DC, Ioannou I (2018) Thermal performance and embodied energy of standard and retrofitted wall systems encountered in Southern Europe, Energy 161: 1016-1027. https://doi.org/10.1016/j.energy.2018.07.124.

[7] Johansson P, Geving S, Hagentoft CE, Jelle BP, Rognvik E, Kalagasidis AS, Time B (2014) Interior insulation retrofit of a historical brick wall using vacuum insulation panels: Hygrothermal numerical simulations and laboratory investigations. Build Environ 79:31-45. https://doi.org/10.1016/j.buildenv.2014.04.014

[8] Künzel HM (1998) Effect of interior and exterior insulation on the hygrothermal behaviour of exposed walls. Mater Struct 31(2):99 -103

[9] Gupta R, Gregg M (2018) Assessing energy use and overheating risk in net zero energy dwellings in UK. Energy Build 158:897-905. https://doi.org/10.1016/j.enbuild.2017.10.061

[10] Govaerts Y, Hayen R, de Bouw M, Verdonck A, Meulebroeck W, Mertens S, Grégoire Y (2018) Performance of a lime-based insulating render for heritage buildings. Constr Build Mater 159:376-389. https://doi.org/10.1016/j.conbuildmat.2017.10.115

[11] Bianco L, Serra V, Fantucci S, Dutto M, Massolino M, (2015) Thermal insulating plaster as a solution for refurbishing historic building envelopes: First experimental results. Energy Build 95:86-91. https://doi.org/10.1016/j.enbuild.2014.11.016

[12] Ibrahim M, Biwole PH, Wurtz E, Achard P (2014) A study on the thermal performance of exterior walls covered with a recently patented silica-aerogel-based insulating coating. Build Environ 81:112-122. https://doi.org/10.1016/j.buildenv.2014.06.017

[13] Stefanidou M (2014) Cement-based renders with insulating properties. Constr Build Mater 65: 427-431. https://doi.org/10.1016/j.conbuildmat.2014.04.062

[14] Palomar I, Barluenga G, Puentes J (2015) Lime–cement mortars for coating with improved thermal and acoustic performance. Constr Build Mater 75: 306-314. https://doi.org/10.1016/j.conbuildmat.2014.11.012

[15] Palomar I, Barluenga G (2017) Assessment of lime-cement mortar microstructure and properties by P- and S- ultrasonic waves. Constr Build Mater 139:334-341. https://doi.org/10.1016/j.conbuildmat.2017.02.083

[16] Palomar I, Barluenga G (2018) A multiscale model for pervious lime-cement mortar with perlite and cellulose fibers. Constr Build Mater 160:136-144. https://doi.org/10.1016/j.conbuildmat.2017.11.032

[17] Terés-Zubiaga J, Martín K, Erkoreka A, Sala JM (2013) Field assessment of thermal behaviour of social housing apartments in Bilbao, Northern Spain. Energy Build 67:118-135. https://doi.org/10.1016/j.enbuild.2013.07.061

[18] Pavlík Z, Vejmelková E, Fiala L, Černý R (2009) Effect of moisture on thermal conductivity of lime-based composites. Int J Thermophys 30 (6):1999-2014. https://doi.org/ 10.1007/s10765-009-0650-y

[19] Khan MI (2002) Factors affecting the thermal properties of concrete and applicability of its prediction models. Build Environ 37(6): 607-614. https://doi.org/10.1016/S0360-1323(01)00061-0

[20] De Freitas VP, Abrantes V, Crausse P (1996) Moisture migration in building walls—Analysis of the interface phenomena. Build Environ 31(2):99-108. https://doi.org/10.1016/0360-1323(95)00027-5

[21] Walker R, Pavía S (2015) Thermal performance of a selection of insulation materials suitable for historic buildings. Build Environ 94(Part 1):155-165. https://doi.org/10.1016/j.buildenv.2015.07.033

[22] Stazi F, Bonfigli C, Tomassoni E, Di Perna C, Munafò P (2015) The effect of high thermal insulation on high thermal mass: Is the dynamic behaviour of traditional envelopes in Mediterranean climates still possible? Energy Build 88:367-383. https://doi.org/10.1016/j.enbuild.2014.11.056

[23] Qin M, Belarbi R, Aït-Mokhtar A, Nilsson LO (2009) Coupled heat and moisture transfer in multi-layer building materials. Constr Build Mater 23(2): 967-975. https://doi.org/10.1016/j.conbuildmat.2008.05.015

[24] Skujans J, Vulans A, Iljins U, Aboltins A (2007) Measurements of heat transfer of multi-layered wall construction with foam gypsum. Appl Therm Eng 27(7):1219-1224. https://doi.org/10.1016/j.applthermaleng.2006.02.047

[25] Bellia L, Minichiello F (2003) A simple evaluator of building envelope moisture condensation according to an European Standard. Build Environ 38(3): 457-468. https://doi.org/10.1016/S0360-1323(02)00060-4

[26] López O, Torres I, Guimarães AS, Delgado JMPQ, de Freitas VP (2017) Inter-laboratory variability results of porous building materials hygrothermal properties. Constr Build Mater 156:412-423. https://doi.org/10.1016/j.conbuildmat.2017.08.184

[27] Lucchi E (2017) Thermal transmittance of historical brick masonries: a comparison among standard data, analytical calculation procedures, and in situ heat flow meter measurements. Energy Build 134:171-184. https://doi.org/10.1016/j.enbuild.2016.10.045

[28] Jiménez MJ, Porcar B, Heras MR (2009) Application of different dynamic analysis approaches to the estimation of the building component U value. Build Environ 44(2):361-367. https://doi.org/10.1016/j.buildenv.2008.03.010

[29] Toman J, Vimmrová A, Černý R (2009) Long-term on-site assessment of hygrothermal performance of interior thermal insulation system without water vapor barrier. Energy Build 41(1):51-55. https://doi.org/10.1016/j.enbuild.2008.07.007

[30] Latif E, Tucker S, Ciupala MA, Wijeyesekera DC, Newport DJ, Pruteanu M (2016) Quasi steady state and dynamic hygrothermal performance of fibrous Hemp and Stone Wool insulations: Two innovative laboratory based investigations. Build Environ 95:391-404. https://doi.org/10.1016/j.buildenv.2015.10.006

[31] Pavlík Z, Černý R (2008) Experimental assessment of hygrothermal performance of an interior thermal insulation system using a laboratory technique simulating on-site conditions. Energy Build 40(5): 673-678. https://doi.org/10.1016/j.enbuild.2007.04.019

[32] Moradias PA, Silva PD, Castro-Gomes JP, Salazar MV, Pires L (2012) Experimental study on hygrothermal behaviour of retrofit solutions applied to old building walls. Constr Build Mater 35:864-873. https://doi.org/10.1016/j.conbuildmat.2012.04.138

[33] Palumbo M, Lacasta AM, Giraldo MP, Haurie L, Correal E (2018) Bio-based insulation materials and their hygrothermal performance in a building envelope system (ETICS). Energy Build 174:147-155. https://doi.org/10.1016/j.enbuild.2018.06.042

[34] Ferrari S, Zanotto V (2013) The thermal performance of walls under actual service conditions: Evaluating the results of climatic chamber tests. Constr Build Mater 43: 309-316. https://doi.org/10.1016/j.conbuildmat.2013.02.056

[35] Strachan PA, Vandaele L (2008) Case studies of outdoor testing and analysis of building components. Build Environ 43(2):129-142. https://doi.org/10.1016/j.buildenv.2006.10.043

[36] UNE-EN ISO 7345 (1996) Thermal insulation. Psychical quantities and definitions. Spanish Organization for Standardization (AENOR)

[37] UNE-EN 1745 (2013) Masonry and masonry products - Methods for determining thermal properties. Spanish Organization for Standardization (AENOR)

[38] UNE-EN ISO 10456 (2007) Buildings materials and products. Hygrothermal properties. Tabulated design values and procedures for determining declared and design thermal values. Spanish Organization for Standardization (AENOR)

[39] Schiavoni S, D'Alessandro F, Bianchi F, Asdrubali F (2016) Insulation materials for the building sector: A review and comparative analysis. Renewable Sustainable Energy Rev 62:988-1011. https://doi.org/10.1016/j.rser.2016.05.045

[40] Pescari S, Tudor D, Tölgyi S, Maduta C (2015) Study concerning the thermal insulation panels with double-side anti-condensation foil on the exterior and polyurethane foam or polyisocyanurate on the interior. Key Eng. Mater 660, 2015: 244–248. https://doi:10.4028/www.scientific.net/KEM.660.244

[41] UNE-EN ISO 13788 (2001) Hygrothermal performance of buildings components and buildings elements. Internal surface temperature to avoid critical surface humidity and interstitial condensation. Calculation method. Spanish Organization for Standardization (AENOR)

[42] BS ISO 9869-1 (2014) Thermal insulation — Building elements — In-situ measurement of thermal resistance and thermal transmittance. Part 1: Heat flow meter method. British Standards Institution (BSI)

[43] Jerman M, Černý R (2012) Effect of moisture content on heat and moisture transport and storage properties of thermal insulation materials. Energy Build 53: 39-46. https://doi.org/10.1016/j.enbuild.2012.07.002

[44] Cabeza LF, Castell A, Medrano M, Martorell I, Pérez G, Fernández I (2010) Experimental study on the performance of insulation materials in Mediterranean construction. Energy Build 42(5):630-636. https://doi.org/10.1016/j.enbuild.2009.10.033

[45] Mazzeo D, Oliveti G, Arcuri N (2016) Influence of internal and external boundary conditions on the decrement factor and time lag heat flux of building walls in steady periodic regime. Appl Energy 164: 509-531. https://doi.org/10.1016/j.apenergy.2015.11.076

[46] Corrado V, Paduos S (2016) New equivalent parameters for thermal characterization of opaque building envelope components under dynamic conditions. Appl Energy 163:313-322. https://doi.org/10.1016/j.apenergy.2015.10.123

[47] Aste N, Leonforte F, Manfren M, Mazzon M, (2015) Thermal inertia and energy efficiency – Parametric simulation assessment on a calibrated case study. Appl Energy 145:111-123. https://doi.org/10.1016/j.apenergy.2015.01.084

List of figures and tables

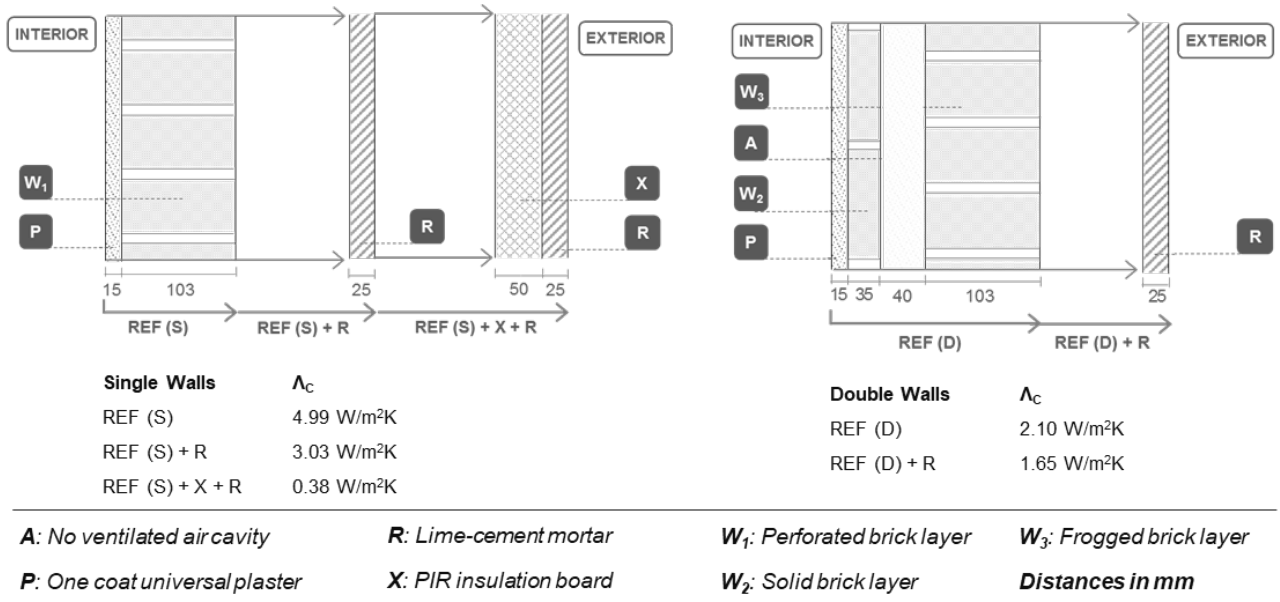

Fig. 1 Vertical cross section of wall layouts (Λ_C = designed thermal conductance)

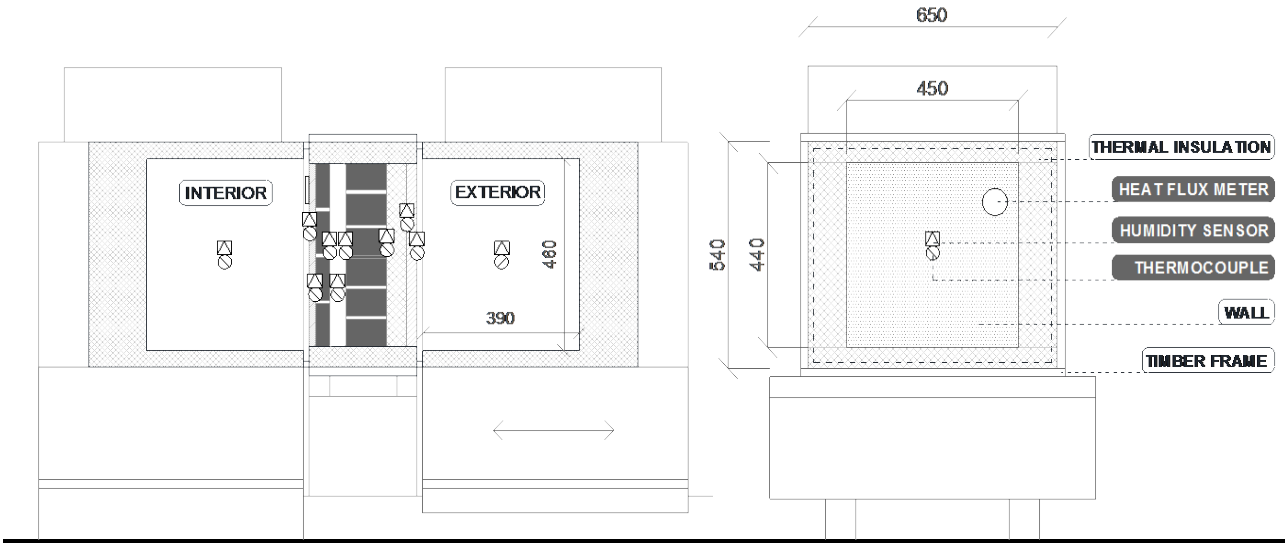

Fig. 2 Experimental setup for climate scenarios simulated using two climate chambers (distance in mm)

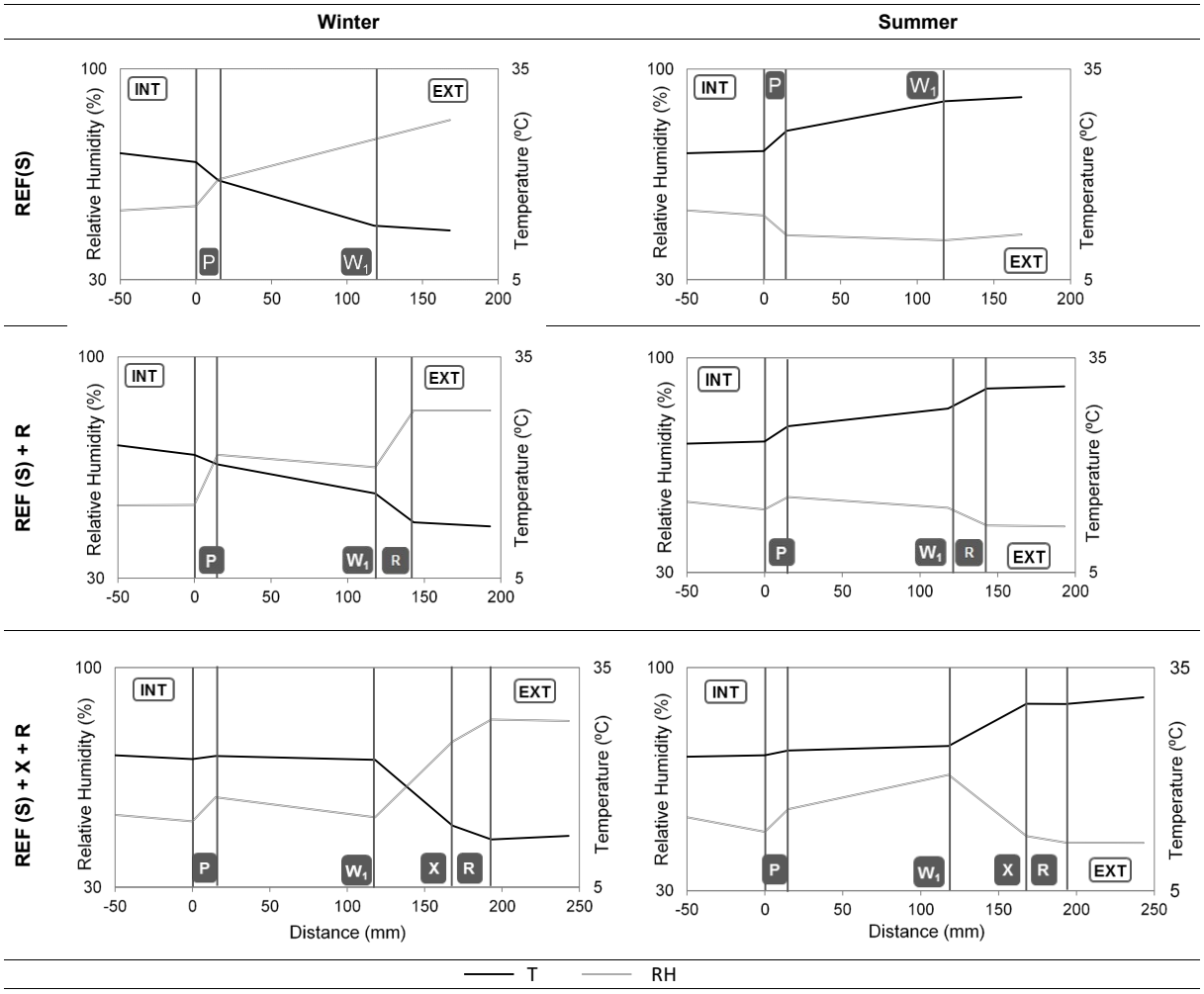

Fig. 3 Temperature and relative humidity cross-section of single walls in steady-state winter and summer scenarios

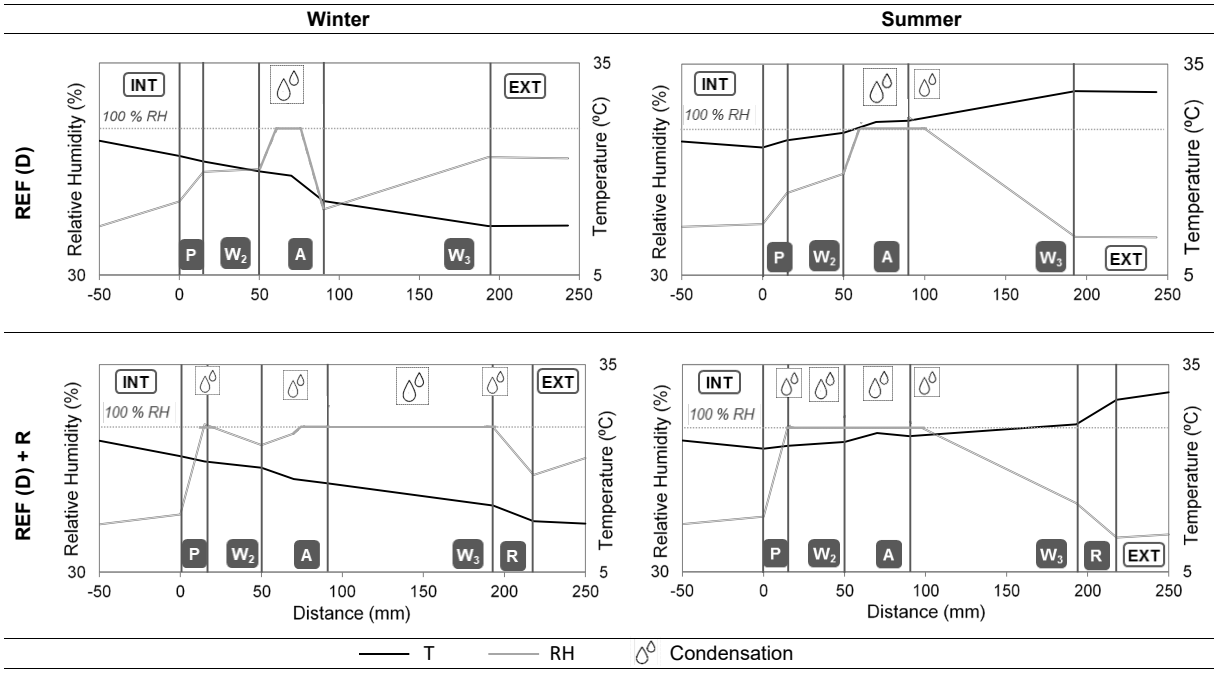

Fig. 4 Temperature and relative humidity cross-section of double walls in steady-state winter and summer scenarios

Table 1 Materials' Properties

		Plaster (P)	Perforated Brick (VPB)[a]	Solid Brick (SB)[a]	Frogged Brick (FB)[a]	Insulation Board (X)[a]	Render (R)
Thickness	mm	15	103	35	103	50	25
ρ	Kg/m^3	1000	1600	2000	1900	30	1800
μ (dry/wet)	-	70 / 6	100 / 50	100 / 50	100 / 50	-	- / 3.40
λ	W/m K	0.24	0.72	0.87	0.51	0.022	0.19
c_p	J/kg K	1000	1000	1000	1000	1400	1000
α	$10^{-7}m^2/s$	2.40	4.50	4.35	2.68	5.24	1.06

ρ - Bulk density; μ - Moisture-dependent water vapor diffusion resistance factor; λ - Thermal conductivity; c_p - Specific heat; α - Thermal diffusivity

[a] Nominal values, provided by the manufacturers.

Table 2 Laboratory measured thermal parameters in winter and summer scenarios

			REF (S)	REF (S) + R	REF (S) + X+ R	REF (D)	REF (D) + R
WINTER	ΔT	° C	-9.06	-9.23	-11.39	-9.86	-9.36
	HF	W/m^2	-50.41	-30.19	-2.20	-20.73	-18.46
	Λ	W/m^2 K	5.56	3.27	0.19	2.10	1.97
	$t_{s,\Delta T}$	h	2.83	6.00	2.00	3.83	3.17
	$t_{s,HF}$	h	4.50	9.00	2.33	8.67	1.67
	CR	-	No	No	No	Yes	Yes
SUMMER	ΔT	° C	6.87	7.39	7.08	8.00	7.11
	HF	W/m^2	31.96	18.93	5.19	13.89	6.19
	Λ	W/m^2 K	4.65	2.56	0.73	1.74	0.87
	$t_{s,\Delta T}$	h	1.50	2.00	2.33	6.50	6.00
	$t_{s,HF}$	h	6.00	12.83	6.00	6.67	18.00
	CR	-	No	No	No	Yes	Yes

ΔT – Temperature difference; HF – Density of heat flux rate; Λ – Thermal conductance; $t_{s,\Delta T}$ – Stabilization time of ΔT; $t_{s,HF}$ – Stabilization time of HF; CR – Condensation risk

Table 3 Temperature, relative humidity and heat flux stabilization time of single and double walls in winter and summer scenarios

			REF (S)		REF (S) + R		REF (S) + X+ R		REF (D)		REF (D) + R	
WINTER			HF		HF		HF		HF		HF	
	Time (h)		4.50		9.00		2.33		8.67		1.67	
			T	RH	T	RH	T	RH	T	RH	T	RH
	S_i	h	3.00	1.33	5.50	4.83	4.33	4.00	7.50	7.50	0.67	1.00
	P- W_1	h	3.50	1.67	9.67	8.00	0.50	4.67	-	-	-	-
	W_1 - R	h	-	-	10.33	6.33	-	-	-	-	-	-
	W_1 - X	h	-	-	-	-	2.67	4.00	-	-	-	-
	X - R	h	-	-	-	-	5.33	13.83	-	-	-	-
	P- W_2	h	-	-	-	-	-	-	9.50	9.33	1.67	10.83
	W_2 - A	h	-	-	-	-	-	-	11.00	x	8.33	6.67
	A	h	-	-	-	-	-	-	12.33	9.83	3.17	0.67
	A- W_3	h	-	-	-	-	-	-	13.83	5.67	4.33	3.00
	W_3 - R	h	-	-	-	-	-	-	-	-	11.50	9.17
	S_e	h	2.00	3.00	6.33	4.33	2.67	3.17	8.33	7.50	7.00	5.33
SUMMER			HF		HF		HF		HF		HF	
	Time (h)		6.00		12.83		6.00		6.67		18.00	
			T	RH	T	RH	T	RH	T	RH	T	RH
	S_i	h	4.50	9.50	6.50	6.00	0.00	0.00	6.50	3.67	12.00	6.00
	P- W_1	h	7.00	14.50	11.00	17.67	7.83	18.00	-	-	-	-
	W_1 - R	h	-	-	12.00	10.33	-	-	-	-	-	-
	W_1 - X	h	-	-	-	-	10.17	12.00	-	-	-	-
	X - R	h	-	-	-	-	3.00	11.83	-	-	-	-
	P- W_2	h	-	-	-	-	-	-	12.50	7.50	16.00	4.17
	W_2 - A	h	-	-	-	-	-	-	12.67	x	18.50	7.17
	A	h	-	-	-	-	-	-	11.00	11.67	24.00	10.50
	A- W_3	h	-	-	-	-	-	-	11.00	1.33	24.00	x
	W_3 - R	h	-	-	-	-	-	-	-	-	22.33	x
	S_e	h	3.00	18.00	6.33	6.00	2.17	4.67	2.67	3.33	12.00	4.83

T – Temperature	RH – Relative Humidity	HF – Density of heat flux rate
P - One coat universal plaster	R - Lime-cement mortar	X - PIR insulation board
W_1 - Perforated brick layer	W_2 - Solid brick layer	W_3 - Frogged brick layer
A - No ventilated air cavity	S_i – Surface interior	S_e – Surface exterior